

Received: 19 November 2018

Revised: 25 January 2019

Accepted: 6 February 2019

DOI: 10.1111/jfbc.12824

FULL ARTICLE

WILEY

Journal of
Food Biochemistry

First report of chromenyl derivatives from spineless marine cuttlefish *Sepiella inermis*: Prospective antihyperglycemic agents attenuate serine protease dipeptidyl peptidase-IV

Soumya Krishnan^{1,2*} | Kajal Chakraborty^{1*}  | Minju Joy¹

¹Marine Biotechnology Division, Central Marine Fisheries Research Institute, Cochin, India

²Department of Biosciences, Mangalore University, Mangalagangothri, India

Correspondence

Kajal Chakraborty, Marine Biotechnology Division, Central Marine Fisheries Research Institute, Ernakulam North, P.B. No. 1603, Cochin, India.

Emails: kajal_cmfri@yahoo.com; kajal.chakraborty@icar.gov.in

Funding information

Indian Council of Agricultural Research, Grant/Award Number: ICAR/HF/2012-2017

Abstract

Spineless marine cuttlefish *Sepiella inermis* has been considered as a popular dietary cephalopod species in Asian and Mediterranean coasts. Bioassay-directed purification of organic extract of *S. inermis* ensued in the characterization of two chromenyl derivatives. The studied compounds exhibited significantly greater antioxidant potencies ($IC_{50} \leq 0.5$ mg/ml) when compared with α -tocopherol. The substituted 1*H*-isochromenyloxy-11-hydroxyethyl pentanoate isoform (compound **1**) efficiently inhibited the carbolytic enzymes along with key regulator of insulin secretion dipeptidyl peptidase-IV (IC_{50} 0.16 mg/ml). The molecular docking simulations displayed optimum binding affinity of the compound **1** (-10.01 kcal/mol) with dipeptidyl peptidase-IV and lesser inhibition constant (K_i 46.41 nM), which along with its permissible hydrophobic-hydrophilic balance ($\log P_{ow} \sim 2$) appeared to play significant roles in its greater antihyperglycemic activity compared to other studied chromenyl isoform. The greater antioxidant and antidiabetic properties of compound **1** could be utilized as an important natural lead against hyperglycemic-related disorders.

Practical applications

The edible spineless marine cuttlefish *Sepiella inermis* are ubiquitously available in Asian and Mediterranean coasts. The sequential chromatographic purification of the organic extract of *S. inermis* led to the identification of two pure chromenyl chemotypes. The metabolites with substituted 1*H*-isochromenyloxy-11-hydroxyethyl pentanoate isoform (compound **1**) displayed potential antioxidative and antihyperglycemic activities compared to the chemotype (**2**) bearing 3*H*-isochromen-5-yl moiety. The attenuating potential of chromenyl chemotype **1** against carbohydrate hydrolyzing enzymes and insulin secretion regulator attributed towards its efficiency as an important natural lead against postprandial hyperglycemia and incretin hormone regulation to maintain glucose homeostasis in the biological system. The chromenyl metabolites isolated from *S. inermis* could be utilized as a functional food ingredient in the nutraceutical formulations against hyperglycemic-related disorders.

KEYWORDS

antihyperglycemic, chromenyl derivatives, dipeptidyl peptidase-IV, molecular docking simulations, *Sepiella inermis*

*The authors have contributed equally.

1 | INTRODUCTION

Diabetes mellitus (type 2 diabetes) is one of the most arduous chronic metabolic syndromes of manifold etiologies distinguished by a failure of glucose homeostasis through disturbances in carbohydrate, protein, and lipid metabolism as a result of impairment in insulin secretion and/or insulin action. According to an assessment of International Diabetes Federation, nearly 366 million people have been affected with diabetes, and it might double by 2,030, whereas in India the diabetic population was found to be 40.9 million, which is predicted to reach up to 60.9 million by 2,025 (Mitra, Dewanjee, & Dey, 2012). The disturbance in the glucose homeostasis arises due to the imbalance between free radicals and antioxidants in cellular system, subsequently resulting in the development of pathogenesis of type 2 diabetes (T2D) (Ullah, Khan, & Khan, 2016). One of the prominent therapeutic approaches to combat T2D is the use of carbohydrate digesting enzyme (α -glucosidase and α -amylase) inhibitors to prolong carbohydrate breakdown time, and thereby reducing postprandial hyperglycemia by retarding glucose absorption rate (Elya et al., 2015). Acarbose is one of the prominent inhibitor of carbohydrate metabolic enzymes in gastrointestinal tract, but it is accompanied by several side effects, such as diarrhea and other intestinal disturbances. Recently, the treatment of T2D is focused on the regulation of incretins or intestinal hormones namely glucose-dependent insulinotropic polypeptide (GIP) and glucagon-like peptide-1 (GLP-1). GLP-1 plays a pivotal role in regulation of blood glucose level by stimulating production of insulin, deterring glucagon secretion, delaying gastric emptying, regulating satiety and stimulating differentiation and regeneration of islet β -cells (Wang et al., 2011). About 50%–60% of total insulin is formed during a meal results from GIP and GLP-1. However, GLP-1 has very short half-lives, approximately for 1–2 min owing to proteolytic cleavage of the N-terminal dipeptide specifically for L-alanine or L-proline at the penultimate position by dipeptidyl peptidase-IV (DPP-IV) into inactive forms. Inhibition of enzyme DPP-IV maintains the level of endogenous active GLP-1 and prolongs its half-life (Purnomo, Soeatmadji, Sumitro, & Widodo, 2015). DPP-IV is a serine protease localized on cellular surfaces. DPP-IV inhibitors are considered to be a safe and unique approach for T2D management, as it retards blood glucose level through regulating hyperglycemia comprising optimum body weight management, improves glycated hemoglobin parameters, and inhibit hypoglycemia (Singh, Jatwa, Purohit, & Ram, 2017). Synthetic peptide-derived DPP-IV inhibitors, namely saxagliptin, sitagliptin, and vildagliptin were approved for T2D management in the western countries, although the durability and long-term safety remained to be proved. Therefore, a systematic research for food based DPP-IV inhibitors from the unexplored marine ecosystem appeared to be of great utility for developing nutraceutical supplements for ameliorating hyperglycemia and other related ailments.

Chromene or chromenone analogues were considered to be significant chemistries of O-heterocyclic compounds with greater pharmacological effects, including antioxidative and antiinflammatory pluralities (Appleton, Sewell, Berridge, & Copp, 2002). The antioxidant and antiinflammatory isochromenone and furanyl-chromenyl

metabolites were identified from estuarine mollusc, *Paphia malabarica* (Joy & Chakraborty, 2017) and bioactive hexahydro-1H-isochromenyl analogues were reported from *Villorita cyprinoides* (Joy & Chakraborty, 2018). Anticancerous hydrogenated chromenone was reported from marine-derived mycelium of *Codium fragile* (El-Beih, Kato, Ohta, & Tsukamoto, 2007) and 6-hydroxy-5-methylramulosin from *Camptotheca acuminata* (Lin et al., 2011). The naturally derived chromenyl compounds with different pharmacologically active substituents have been vital for the development of nutraceutical and functional supplements.

Landing and consumption of cephalopods have increased in the last few decades due to their prominent nutritive values and various biological activities (Chakraborty & Joy, 2016; Ramasamy et al., 2012). The cuttlefishes belonging to Sepiidae inhabit in the tropical or temperate oceanic waters, and are important seafood items at Mediterranean, East Asian, and English Channel coasts. Among the cuttlefishes, *Sepiella inermis* (spineless cuttlefish) forms a commercially important fishery in Thailand, India, and Sri Lanka, and is also targeted by small-scale fisheries, for example in Indo-Chinese waters (Reid, Jereb, & Roper, 2005). From the nutritional point of view, *S. inermis* has been considered to be a rich source of long-chain polyunsaturated fatty acids, proteins, well-balanced vitamins and essential minerals (Chakraborty, Joy, & Vijayagopal, 2016). Earlier report of literature from our laboratory reported the free radical scavenging and antidiabetic activities of crude extract from the edible tissues of this particular species (Chakraborty & Joy, 2016). As a continuing program to investigate bioactive chromenyl analogues from the economically important seafood species, the ethyl acetate-methanol (EA-MeOH) extract of *S. inermis* was partitioned by sequential chromatographic fractionation to obtain two chromenyl derivatives. Their structures were elucidated using Fourier transform infrared (FTIR), nuclear magnetic resonance (NMR), and mass spectroscopic analyzes. The chromenyl analogues identified in the present study were assessed for antioxidant activities by 2, 2-diphenyl-1-picrylhydrazyl (DPPH) and 2, 2'-azino-bis (3-ethylbenzothiazoline-6-sulfonic acid) (ABTS⁺) scavenging assessments. The inhibitory properties of the studied compounds against the catalytic enzymes α -glucosidase and α -amylase along with key regulator of insulin secretion dipeptidyl peptidase-IV (DPP-IV) were examined to recognize the utilization potential of these natural leads against hyperglycemic-related disorders. Structure-bioactivity inter-relationships of the chromenyl derivatives were examined by different physico-chemical characteristics of the studied chromenyl isoforms. The modes of inhibition of DPP-IV by the compounds were determined by *in silico* molecular docking simulations.

2 | MATERIALS AND METHODS

2.1 | Sample collection and preparation of crude organic extracts

The specimens of *S. inermis* (5.5 kg) were collected freshly from the landing center of Arabian Sea located at Lat 8°48' N, Long 78°9' E; Lat 9°14' N, Long 79°14' E, along the Southwestern coast of

Indian subcontinent. The species was washed to eliminate the dirt and mucus remains. The visceral organs, including ink-gland were judiciously separated from the edible part of the species. The edible portion were homogenated and freeze dried using a lyophilizer (Labogene Scanvac Cool Safe, Denmark) yielding the freeze-dried powder (1890 g, yield 34.36%). The lyophilized powder was then extracted in the solvent EA-MeOH (1:1, v/v, 1,500 ml × 2) using sonication (7 hr) in the presence of nitrogenous atmosphere. The crude organic fraction was separated from species residue through filtration by Whatman-1 filter paper in the presence of anhydrous sodium sulfate (Na₂SO₄), and the filtrate was concentrated by utilizing a rotary evaporator (55°C; Heidolf, Germany) to yield the crude organic extract of *S. inermis* (64 g, yield 3.38% on dry weight basis).

2.2 | Chromatographic partitioning

The crude organic (EA-MeOH) extract of *S. inermis* (64 g) was repetitively partitioned utilizing column chromatography. The crude extract was mixed with 60–120 mesh sized coarse silica (6 g) and packed into an open glass column (110 cm × 5 cm) charged with silica gel (60–120 mesh, 80 g). The column was initially eluted with *n*-hexane and the solvent system increased by EA and MeOH, to yield six column fractions (SI₁ through SI₆). The bioactive properties of the column fractions SI₁₋₆ were assessed, and SI₅ was preferred for further purification due to their higher antidiabetic activity against DPP-IV (IC₅₀ 0.74 mg/ml) and free radical potencies (IC₅₀ < 0.85 mg/ml) (Table S1). The fraction SI₅ (12.75 g; 19.92%) was further purified by vacuum-liquid chromatographic experimentation on the column (46 cm × 4 cm) with 230–400 meshed fine silica using increasing polar gradient of *n*-hexane/chloroform (CHCl₃)/MeOH to obtain 18 fractions (30 ml each), which were pooled to eight subgroups (SI_{5.1}–SI_{5.8}) after thin layer chromatographic (TLC) (CHCl₃:MeOH, 8:2 v/v) analyses. The subfraction SI_{5.7} (40% MeOH:CHCl₃; 2,310 mg; 18.04%) displayed greater bioactive potencies against DPPH and DPP-IV (IC₅₀ < 0.6 mg/ml) when compared with other subfractions, and hence was considered for purification of bioactives. The fraction SI_{5.7} was purified using preparative reversed-phase high-pressure liquid chromatography (RP-HPLC, C₁₈-1.4 cm × 25 cm, 5 μm) with acetonitrile (MeCN)/MeOH (90:10 v/v; 10 ml/min) to yield compounds **1** (R_t 11.2 min, 92 mg) and **2** (R_t 17.1 min, 126 mg), which were found to be homogeneous in TLC (CHCl₃/MeOH, 80:20 v/v) and RP-HPLC (MeOH:MeCN, 10:90 v/v).

2.3 | Spectroscopic characterization of the purified compounds

NMR spectroscopic experiments, such as proton NMR (¹H NMR), carbon NMR (¹³C NMR), along with two-dimensional proton correlation spectroscopy (¹H-¹H COSY) and heteronuclear multiple-bond correlation spectroscopy (HMBC) were conducted with a Bruker Avance DPX 500 NMR spectrometer using an internal standard (tetramethylsilane) (Bruker, Karlsruhe, Germany), whereas the compounds were dissolved in deuterated chloroform (CDCl₃). NMR spectral

analyses were carried with MestReNova version 7.1.1-9649© 2012 (Mestrelab Research, S.L., Spain). FTIR spectral data were recorded on FTIR spectrophotometer (Perkin-Elmer 2000, USA) between 4,000 and 400 cm⁻¹ scan range (Perkin-Elmer, MA, USA). Ultra-violet (UV) spectral data were recorded with a ultra-violet (UV-VIS) spectrophotometer (AquaMate-8000, Thermo Scientific, USA). Gas-chromatographic mass-spectroscopic (GC-MS) experiments were conducted on a Perkin-Elmer instrument (Clarus-680, MA, USA) by electronic-impact ionization mode, and the components resolved by a capillary column (Elite-5; 50 m × 220 μm i.d., 0.25 μm film).

2.3.1 | 11-(3,4,4a,5,8,8a-Hexahydro-8-methoxy-4-methyl-1*H*-isochromen-4-yloxy)-11-hydroxyethyl pentanoate (1)

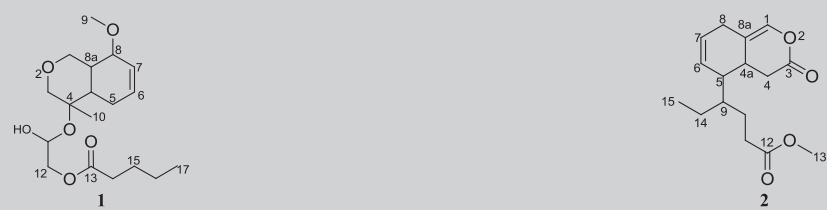
Brown oily; UV λ_{max} MeOH (log ε 2.42): 254 nm; [α]_D²⁶ -19.9° (CHCl₃, c0.014); TLC (silica GF-254; CHCl₃/MeOH, 80:20 v/v) R_f: 0.37; R_t (RP-C₁₈ HPLC, Shimadzu, Japan; C₁₈ 25 cm × 0.46 cm, 5 μm; MeOH:MeCN, 10:90 v/v): 2.737 min (Fig. S1); IR (cm⁻¹) (stretching ν, bending δ, rocking ρ): 3,445 (br, O-Hν), 2,924, 2,855 (C-Hν), 1,730 (C=Oν), 1,476, 1,386 (C-Hδ), 1,233 (C-Hρ), 1,088 (C-O-Cν), 971 (=C-Hδ). ¹H NMR (500 MHz, CDCl₃): δ 5.37 (1H, t, 5.3Hz), 5.35 (1H, q, 4.0Hz), 5.21 (1Hα, t), 4.39 (1Hα, d), 4.14 (1Hβ, d), 3.93 (2H, d), 3.73 (2H, s), 3.38 (1Hα, t), 3.29 (3H, s), 2.30 (2H, t), 2.19 (1Hβ, t), 2.09 (1Hβ, t), 2.03 (2H, t), 1.58 (2H, m), 1.29 (2H, s), 1.27 (3H, s), 0.89 (3H, t); ¹³C NMR (125 MHz, CDCl₃): δ 173.64, 129.99, 129.69, 70.42, 70.36, 69.12, 66.24, 63.55, 62.97, 54.34, 34.15, 31.94, 29.78, 29.39, 27.24, 24.92, 22.70 14.12; ¹H-¹H COSY and HMBC data were given in Table 1. EIMS: found *m/z* 342.2048 [M]⁺, cal. for C₁₈H₃₀O₆ 342.2042 (Δ = 1.7 ppm).

2.3.2 | Methyl 9-(4,4a,5,8-tetrahydro-3-oxo-3*H*-isochromen-5-yl)hexanoate (2)

Dark yellow oily; UV λ_{max} MeOH (log ε 2.24): 198 nm; [α]_D²⁶ -21.3° (CHCl₃, c0.015); TLC (silica GF-254; CHCl₃/MeOH, 80:20 v/v) R_f: 0.49; R_t (RP-C₁₈ HPLC; MeOH:MeCN, 10:90 v/v): 4.38 min (Figure S2); IR (cm⁻¹): 2,925, 2,856 (C-Hν), 1,732 (C=Oν), 1,396 (C-Hδ), 1,228 (C-Hρ), 1,085, 1,053 (C-O-Cν), 969, 924 (=C-Hδ). ¹H NMR (500 MHz, CDCl₃): δ 6.20 (1H, s), 5.37 (1H, dt, 5.3, 2.0 Hz), 5.35 (1H, t, 2.2Hz), 3.65 (3H, s), 2.83 (2H, d), 2.81(1Hβ, t), 2.37 (2H, d), 2.29 (2H, t), 2.06 (1Hβ, t), 1.97 (1Hα, m), 1.60 (2H, q), 1.27 (2H, m), 0.86 (3H, t); ¹³C NMR (125 MHz, CDCl₃): δ 174.43, 173.60, 132.03, 129.32, 128.56, 127.86, 51.44, 39.78, 34.11, 31.91, 29.67, 25.62, 24.95, 22.68, 20.54, 14.1; ¹H-¹H COSY and HMBC data were given in Table 1. EIMS: found *m/z* 278.1522 [M]⁺, cal. for C₁₆H₂₂O₄ 278.1518 (Δ = 1.4 ppm).

2.4 | Antioxidant and antidiabetic activities

The antioxidant properties of the studied chromenyl analogues (**1-2**) isolated from *S. inermis* were resolved by in vitro DPPH and

TABLE 1 NMR spectroscopic data (in CDCl₃)^{a,b} of chromenyl compounds, **1-2** isolated from *S. inermis*


C. No.	¹³ C	¹ H(int.,mult.,J in Hz) ^b	¹ H- ¹ H COSY	HMBC	C. No.	¹³ C	¹ H(int.,mult.,J in Hz) ^b	¹ H- ¹ H COSY	HMBC
1	63.55	3.93(2H,d)	H-8a	C-3,4,8a	1	128.56	6.20(1H,s)	-	C-3,8a
2	-	-	-	-	2	-	-	-	-
3	66.24	3.73(2H,s)	-	C-4	3	173.60	-	-	-
4	69.12	-	-	-	4	31.91	2.37(2H,d)	H-4a	C-3
4a	31.94	2.09(1Hβ,t)	H-8a	C-3,4	4a	39.78	2.81(1Hβ,t)	H-5	C-3,6,8a
5	27.24	2.03(2H,t)	H-6	C-6,7,8a	5	20.54	2.06(1Hβ,t)	H-6, H-9	C-6,7,9
6	129.69	5.35(1H,q,4.0Hz)	-	C-5,4a	6	132.03	5.35(1H,t,2.2Hz)	-	C-5,7,8,9
7	129.99	5.37(1H,t,5.3Hz)	H-8	-	7	127.86	5.37(1H,dt,5.3,2.0Hz)	H-8	C-6,8a
8	70.36	3.38(1Hα,t)	H-8a	C-9	8	25.62	2.83(2H,d)	-	C-6,7,8a
8a	29.39	2.19(1Hβ,t)	-	C-4a,5,7	8a	129.32	-	-	-
9	54.34	3.29(3H,s)	-	C-8	9	29.67	1.97(1Hα,m)	H-10, H-14	C-5,6,12
10	29.78	1.27(3H,s)	-	C-4,4a	10	24.95	1.60(2H,q)	H-11	C-9,11,12
11	70.42	5.21(1Hα,t)	H-12	C-4,12	11	34.11	2.29(2H,t)	-	C-12
12	62.97	4.14(1Hβ,d) 4.39(1Hα,d)	-	C-11,13	12	174.43	-	-	-
13	173.64	-	-	-	13	51.44	3.65(3H,s)	-	C-12
14	34.15	2.30(2H,t)	H-15	C-13,15	14	22.68	1.27(2H,m)	H-15	C-9,15
15	24.92	1.58(2H,m)	H-16	C-13,14,16	15	14.10	0.86(3H,t)	-	C-9,14
16	22.70	1.29(2H,m)	H-17	C-15,17	-	-	-	-	-
17	14.12	0.89(3H,t)	-	C-16,14	-	-	-	-	-

Note. Assignments were made with the aid of ¹H-¹H COSY, HSQC, HMBC, and NOESY experiments.

^aNMR spectra recorded using Bruker AVANCE III 500 MHz (AV 500) spectrometers. ^bValues in ppm, multiplicity, and coupling constants (*J* = Hz) are indicated in parentheses.

ABTS⁺ (Odeleye et al., 2016; Wojdylo, Oszmianski, & Czemyers, 2007) radical-scavenging analyses. Antidiabetic potential of the titled compounds were assessed using the dipeptidyl peptidase-IV enzyme (DPP-IV, human recombinant) inhibitory potential (Kojima, Ham, & Kato, 1980) as well as the inhibition capability toward the carbolytic enzymes α -amylase (procured from porcine pancreas) and α -glucosidase (from yeast), according to the method described earlier (Hamdan & Afifi, 2004). The results were expressed as 50% inhibitory concentration (IC₅₀, in mg/ml), which was obtained from the graph plotted with concentrations of sample against percentage inhibition toward enzyme/radical.

2.5 | Structure-bioactivity interrelationship analysis

The molecular physicochemical characteristics, such as hydrophobic (logarithmic value of octanol/water partition coefficient, log *P*_{ow}), polar (polarizability PI and topological polar surface area

tPSA), and bulk (Pr parachor, MR molar refractivity, and MV molar volume) (Joy & Chakraborty, 2018) parameters were used to study the structure-bioactivity interrelationship analysis of the chromenyl derivatives. These parameters were deduced by ACD (Advanced Chemistry Development) ChemSketch (version 12.0; Canada) and ChemDraw Ultra (version 12.0; Cambridge Soft Corporation, MA, USA) programs.

2.6 | In silico molecular docking analysis

In silico molecular docking analyses of the purified chromenyl analogues were demonstrated by utilizing the docking software (Autodock 4.0, version 1.5.6), to establish the stable ligand-protein conformation. The studied compounds were drawn with Chemsketch software (version 3.5) and saved as MDL-molfiles, and finally converted to PDB format with Open Babel GUI (version 2.4.1). The crystal structure of DPP-IV (PDB: 3F8S; resolution 2.0 Å) (Ammirati et

al., 2009) was obtained from RCSB-protein databank, wherein the water molecules were excluded from target proteins, and Swiss-PdbViewer (SPDBV v4.1.0) was utilized for the energy minimization of enzyme. Molecular docking studies of the ligands were performed to evaluate the optimum binding modes between the DPP-IV active sites and the studied metabolites. The docking studies were performed using AutoDock 4 (AutoDock Tools version 1.5.6) and bound ligands, cofactors and water were removed. The target enzyme was accounted for partial atomic Kollman charges designation, and polar hydrogens. Torsion bonds of the studied chromenyl analogues were chosen and defined, wherein the 3D-grid box was created by Auto-Grid calculation to calculate the coupling energies on the DPP-IV coordinates. Grid map set values for docking of DPP-IV were selected as $x = 8.512$, $y = 5.755$, $z = 52.694$ ($58 \text{ \AA} \times 66 \text{ \AA} \times 66 \text{ \AA}$) points. Running of the docking calculation was demonstrated by utilizing Cygwin-1/Cygwin-2, and root-mean-square deviation to assess lowest binding energy. USCF chimera 1.11.2 (University of California, San Francisco-UCSF) programming was employed for visual representation of results to recognize H-bonding relations between the designated chromenyl derivatives and target DPP-IV.

2.7 | Statistical analysis

The statistical software SPSS (Statistical Program for Social Sciences, version 13.0; USA) was utilized to ascertain the significant difference using ANOVA (one-way analysis of variance) between means. The results were presented as the mean of replicate experiments with 5% level of significance ($p \leq 0.05$).

3 | RESULTS AND DISCUSSION

3.1 | General

The marine cephalopods belonging to the family Sepiidae represent a prominent share in the fishery sector, and were designated to possess different bioactive metabolites with respect to various pharmacological activities (Chakraborty & Joy, 2016). The present study deals with isolation of bioactive chromenyl analogues from the EA-MeOH extract of spineless cuttlefish *S. inermis* using extensive spectroscopic techniques. The bioactive properties of the isolated chromenyl analogues with respect to their antioxidant and antidiabetic activities using in vitro pharmacological models were assessed.

3.2 | Chromatographic fractionation and structural characterization of chromenyl derivatives from *S. inermis*

The crude EA-MeOH extract of *S. inermis* was firstly fractionated to five key sub-fractions (SI_1 – SI_6), and among which SI_5 displayed significantly greater recovery (20%) than SI_1 through SI_3 and SI_6 (< 20%). The sub-fractions, SI_5 also exhibited higher antioxidant (IC_{50}^{DPPH} scavenging 0.84 mg/ml; IC_{50}^{ABTS} scavenging 0.82 mg/ml) and antidiabetic (IC_{50}^{DPP-IV} inhibitory 0.74 mg/ml) properties than those displayed by

others ($IC_{50} > 0.80$ mg/ml) (Table S1). Therefore, SI_5 was selected for downstream chromatographic purification to obtain two chromenyl derivatives (1–2). The structures of the studied compounds were interpreted by inclusive spectroscopic techniques (Figure 1).

3.2.1 | 11-(3,4,4a,5,8,8a-Hexahydro-8-methoxy-4-methyl-1H-isochromen-4-yloxy)-11-hydroxyethyl pentanoate (1)

The hexahydro isochromenyl analogue, 11-(hexahydro-8-methoxy-4-methyl-1H-isochromen-4-yloxy)-11-hydroxyethyl pentanoate (1) was sequentially fractionated as brown oily through repeated chromatographic purifications. The mass spectrum envisaged the occurrence of its molecular ion peak at m/z 342, which supported the molecular formula of the titled compound as $C_{18}H_{30}O_6$ through the broad IR/NMR analyses (Table 1, Figures S3–S11). The four degrees of unsaturations were deduced to correspond toward two double bonds and two ring systems. The absence of aromatic protons (δ 6.5–8.5) signified the absence of aromatic rings in the structure. The distortionless enhancement by polarization transfer (DEPT₁₃₅) and ^{13}C shift resonances displayed 18 carbons, which include one ester carbonyl (δ 173.64), alkenic carbons (δ 129–130), one hydroxylated carbon (δ 70.36), four oxygenated carbons [δ 63.55, 66.24, 69.12 (quaternary carbon), 54.34 (–OCH₃) and 62.97 [–C(=O)–O–CH₃]] along with shielded methyls, methylenes, and methines in the range of δ 34–14. The one-dimensional NMR resonances along with heteronuclear single quantum coherence spectroscopy (HSQC) (Figure S7) suggested the possibilities of one methylene of oxygenated end

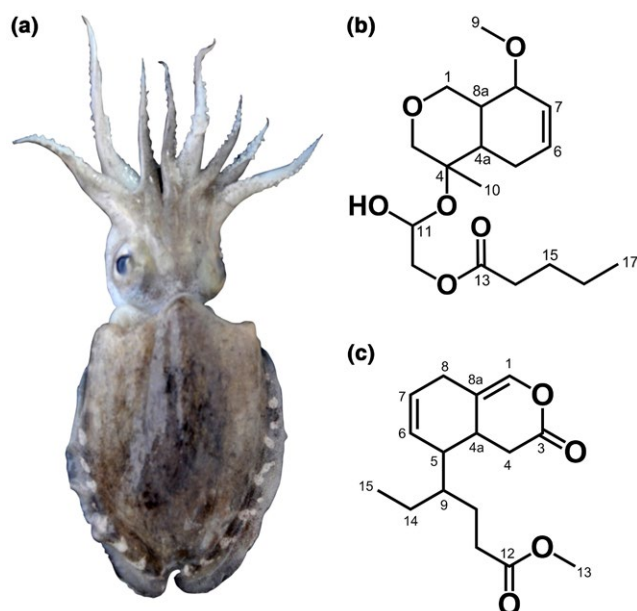


FIGURE 1 (a) Photographic representation of *S. inermis* (spineless cuttlefish). Structural representations of the chromenyl analogues, (b) 11-(hexahydro-8-methoxy-4-methyl-1H-isochromen-4-yloxy)-11-hydroxyethyl pentanoate (compound 1) and (c) methyl 9-(tetrahydro-3-oxo-3H-isochromen-5-yl)hexanoate (compound 2) purified from *S. inermis*

of ester group (δ H 4.14, 4.39/ δ C 62.97), one methylene of carbonyl end of ester group (δ H 2.30/ δ C 34.15), one disubstituted sp^2 alkene (δ H 5.35/ δ C 129.69; δ H 5.37/ δ C 129.99); two oxygenated methylenes (δ H 3.93/ δ C 63.55; δ H 3.73 singlet/ δ C 66.24); one each of oxygenated methine (δ H 3.38/ δ C 70.36), oxygenated methyl (δ H 3.29/ δ C 54.34) and deshielded hydroxylated methine (δ H 5.21/ δ C 70.42). The presence of oxygenated singlet methylene at δ H 3.73 and oxygenated methylene at δ H 3.93 with doublet splitting suggested that these groups might be shared by a common oxygen atom and the proton at δ H 3.93 was assigned at H-1 position. The ^1H - ^1H COSY correlations suggested two spin systems in the oxygenated bicyclic ring, which were found to be δ H 3.93 (attributed to H-1)/2.19 (H-8a)/3.38 (H-8)/5.37 (H-7) including δ H 2.09 (H-4a)/2.19 (H-8a) and δ 2.03 (H-5)/5.35 (H-6) that supported the basic skeleton of hexahydro isochromenyl ring (Figure 2A, S6). This oxygen-enclosed hexahydro isochromenyl ring was further established with the help of long-range HMBCs from δ 3.93 (H-1) to δ 29.39 (C-8a); δ 2.03 (H-5) to δ 129.69 (C-6), 129.99 (C-7), 29.39 (C-8a); δ 5.35 (H-6) to δ 27.24 (C-5) and δ 2.19 (H-8a) to δ 31.94 (C-4a), 129.99 (C-7), 27.24 (C-5) (Figure 2A, S8). Also, the position of oxygenated singlet methylene at

δ H 3.73 (assigned to H-3) and its attachment to the oxygenated quaternary carbon at δ 69.12 (C-4) in the hexahydro isochromenyl ring were confirmed by the HMBC relations from δ 3.73 (H-3) to δ 69.12 (C-4); δ 2.09 (H-4a) to δ 66.24 (C-3), 69.12 (C-4) and δ 3.93 (H-1) to δ 66.24 (C-3), 69.12 (C-4). An oxygenated deshielded singlet signal at δ 3.29 with an integral of three suggested the presence of methoxy group, and its attachment to the basic hexahydro isochromenyl ring were suggested by the HMBCs from δ 3.29 (H-9) to δ 70.36 (C-8) and δ 3.38 (H-8) to δ 54.34 (C-9). The hexahydro-1*H*-isochromene part of pericoannosin A was similar to the studied compound (Zhang et al., 2015). The reported compound enclosed a trisubstituted alkene and side chains at C-1 and C-3 positions, whereas the studied compound enclosed a disubstituted alkene and side chains at C-4 and C-8 positions. An upfield singlet signal at δ H 1.27 (proton integral of three; δ C 29.78, HSQC) was exhibited by its HMBC correlations with the carbon traces at δ 69.12 (C-4), 31.94 (C-4a), which supported the direct attachment of methyl to the quaternary carbon enclosed in the bicyclic ring. The COSY relations between the protons at δ 5.21 (H-11)/4.14, 4.39 (H-12) and δ 2.30 (attributed to H-14)/1.58 (H-15)/1.29 (H-16)/0.89 (H-17) established a side chain with ester linkage. The HMBC couplings from δ 5.21 (H-11) to δ 62.97 (C-12); δ 4.14 (H-12) to δ 70.42 (C-11), 173.64 (C-13); δ 2.30 (H-14) to δ 173.64 (C-13), 24.92 (C-15); δ 1.58 (H-15) to δ 173.64 (C-13), 34.15 (C-14), 22.70 (C-16); δ 1.29 (H-16) to δ 24.92 (C-15), 14.12 (C-17) and δ 0.89 (H-17) to δ 22.70 (C-16), 34.15 (C-14) appropriately supported the presence of hydroxyethyl pentanoate chain. The attachment of hydroxyethyl pentanoate chain at C-4 (δ 69.12) was confirmed by the HMBC from δ 5.21 (H-11) to δ 69.12 (C-4). The comparatively lesser coupling constants of 4.0 and 5.3 Hz were found to correspond toward the protons at δ 5.35 (H-6) and δ 5.35 (H-7), respectively. The later established that the disubstituted alkene was oriented as *cis* (*Z*) in the hexahydro isochromenyl ring system. The stereochemical orientations of the chiral centers at C-4, C-4a, C-8, and C-8a were ascribed through the detailed nuclear overhauser effect spectroscopy (NOESY) experiments (Figure 2B, S9). The NOESY resonances among δ 2.09 (H-4a), 4.14 (H- β -12) and δ 2.19 (H-8a) suggested their equal plane of symmetry, and were arbitrarily aligned as β -protons. Thus, the *cis* orientation of ring junction of hexahydro isochromenyl framework was established, and the α -disposition of the hydroxyethyl pentanoate chain at C-4 was confirmed. The NOESY couplings between the protons at δ 3.38 (H-8), 4.39 (H- α -12), and 5.21 (H-11) suggested their equal plane of symmetry, and these did not display any NOESY correlations with the β -aligned protons, therefore, assigned as α -oriented protons. Thus, the β -orientation of hydroxyl group at C-11 and methoxyl group at C-8 were appropriately assigned (Figure S9). The basic hexahydro-isochromenyl skeleton of the studied compound isolated from *S. inermis* was similar to hexahydro-isochromenyl-meroterpenoids that was previously reported from the mollusc, *V. cyprinoides* (Joy & Chakraborty, 2018). The IR spectrum of compound 1 exhibited the stretching absorptions at 2,924–2,855, 1,730 and 3,445 cm^{-1} , that denoted the presence of alkanes, ester carbonyl, and hydroxyl moieties, respectively (Figure S10). The molecular ion peak at m/z 342 ($[\text{M}]^+$) was found to undergo

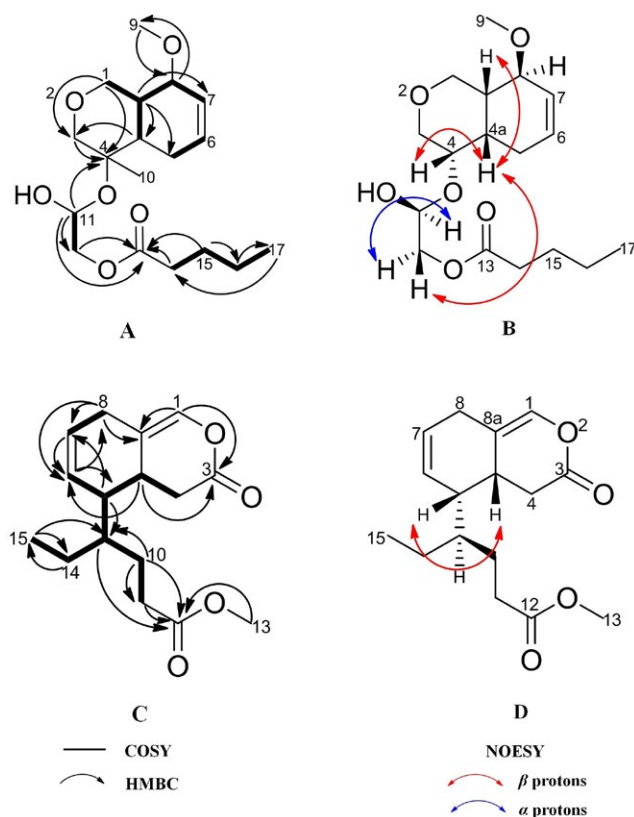


FIGURE 2 (A) ^1H - ^1H COSY, HMBC and (B) NOESY correlations of 11-(hexahydro-8-methoxy-4-methyl-1*H*-isochromen-4-yl)oxy)-11-hydroxyethyl pentanoate (compound 1) and (C and D) methyl 9-(tetrahydro-3-oxo-3*H*-isochromen-5-yl)hexanoate (compound 2). The key ^1H - ^1H COSY couplings were represented in bold-face bonds. The key HMBC couplings have been represented by the double-barbed arrow. The NOESY relations were represented by double sided arrows, wherein the red and blue colored arrows indicated the beta (β -) and alpha (α -) protons, respectively

McLafferty rearrangement with the elimination of propene to yield 11-(hexahydro-8-methoxy-4-methyl-isochromen-4-yloxy)-11-hydroxyethoxy)ethanol fragment at m/z 300 (**1B**) (Figures S11–S12). The fragment at m/z 300 (**1B**) underwent McLafferty rearrangement to afford the base peak at m/z 60 (**1D**, acetic acid) along with a fragment at m/z 240 (**1C**). The latter underwent McLafferty rearrangement, which could result in the formation of the base peak at m/z 60 (**1E**, acetic acid) along with an ion peak at m/z 180. The elimination of one methoxy radical from the fragment at m/z 180 yielded tetrahydro-4-methyl-1*H*-isochromene fragment with m/z 149 (**1G**). The repeated elimination of $C_3H_4^{\bullet\bullet}$ and 3 methyl radicals from the ion at m/z 149 yielded the fragments at m/z 112 (**1H**, attributed to 3,6-dihydro-3,4-dimethyl-2*H*-pyran) and m/z 70 (**1J**, attributed to vinyloxy ethene), respectively.

3.2.2 | Methyl 9-(4,4a,5,8-tetrahydro-3-oxo-3*H*-isochromen-5-yl)hexanoate (2)

The previously undisclosed tetrahydro oxo-isochromenyl derivative, named as methyl 9-(4,4a,5,8-tetrahydro-3-oxo-3*H*-isochromen-5-yl)hexanoate (**2**) was isolated through the repetitive chromatographic fractionations, as dark yellow colored oily compound. The mass spectrum demonstrated a molecular ion peak at m/z 278, and exhaustive IR/NMR analyses suggested its molecular formula as $C_{16}H_{22}O_4$ (Table 1, Figures S13–S21). The degrees of unsaturations were found to be five, which comprised of three double bonds including one carbonyl and two cyclic systems. The DEPT along with ^{13}C NMR resonances suggested the occurrences of 15 carbon atoms including those belonging to two esters (δ 173–174), alkenic (δ 127–132), one oxygenated end of methyl carbon of ester [δ 51.44 [–C(=O)–O–CH₃]] along with shielded methyls, methylenes, and methines (at δ 14–40). The $^1H/^{13}C$ NMR along with HSQC confirmed the probabilities of one each of methyl group at oxygenated end of ester (δH 3.65/ δC 51.44), methylene at carbonyl end of ester (δH 2.29/ δC 34.11), disubstituted sp^2 alkene (δH 5.35/ δC 132.03; δH 5.37/ δC 127.86); and trisubstituted sp^2 alkene (δC 129.32; δH 6.20/ δC 128.56) (Figure S17). The greatly deshielded singlet proton trace at δ 6.20 exhibited HSQC correlation with the carbon at δ 128.56 (arbitrarily positioned at C-1) suggesting that it was not a part of any aromatic group. This signal might be related to an alkene, which was positioned between the highly electron withdrawing groups, such as ester. The HMBC couplings from δ 6.20 (H-1) to δ 173.60 (C-3) and 129.32 (C-8a) further supported that the proton at δ 6.20 was directly bonded to the oxygenated end of carboxylate group, which was the part of an ester enclosed bicyclic ring system. The $^1H-^1H$ COSY couplings displayed two spin systems in the carboxylated bicyclic ring, which were δH 2.37 (attributed to H-4)/2.81 (H-4a)/2.06 (H-5)/5.35 (H-6) including δH 5.37 (H-7)/2.83 (H-8) that supported the partial skeleton of tetrahydro oxo-isochromenyl ring framework (Figure 2C, S16). This was further corroborated through the long range HMBC couplings from δ 2.37 (H-4) to δ 173.60 (C-3); δ 2.81 (H-4a) to δ 173.60 (C-3), 132.03 (C-6), 129.32 (C-8a); δ 2.06

(H-5) to δ 132.03 (C-6), 127.86 (C-7); δ 5.35 (H-6) to δ 20.54 (C-5), 127.86 (C-7), 25.62 (C-8); δ 5.37 (H-7) to δ 132.03 (C-6), 129.32 (C-8a) and δ 2.83 (H-8) to δ 132.03 (C-6), 127.86 (C-7), 129.32 (C-8a) (Figure 2C, S18). The carboxylate enclosed bicyclic ring skeleton could be comparable to the tetrahydro-isochromenone analogue isolated from yellow-foot mollusc *Paphia malabarica* (Joy & Chakraborty, 2017). The COSY correlations from δ 1.97 (H-9)/1.60 (H-10)/2.29 (H-11) including δ 1.97 (H-9)/1.27 (H-14)/0.86 (H-15) were supported by the HMBs from δ 1.97 (H-9) to δ 174.43 (C-12); δ 1.60 (H-10) to δ 174.43 (C-12), 29.67 (C-9); δ 2.29 (H-11) to δ 174.43 (C-12); δ 3.65 (H-13) to δ 174.43 (C-12); δ 1.27 (H-14) to δ 29.67 (C-9), 14.10 (C-15) and δ 0.86 (H-15) to δ 29.67 (C-9), which established the partial structure of methyl hexanoate side chain. The attachment of methyl hexanoate side chain to tetrahydro oxo-isochromenyl ring at C-5 was established with the help of COSY interaction from δ 2.06 (H-5)/1.97 (H-9) and long range HMBs from δ 2.06 (H-5) to δ 29.67 (C-9); δ 5.35 (H-6) to δ 29.67 (C-9); δ 1.97 (H-9) to δ 20.54 (C-5), 132.03 (C-6). The relatively lesser coupling values of 2.2 and 5.3 Hz for the protons at δ 5.35 (H-6) and δ 5.35 (H-7), respectively, suggested their *cis* (*Z*) orientation in the tetrahydro oxo-isochromenyl system. The stereochemical orientations of chiral centers at C-4a, C-5, and C-9 were established through NOESY resonances (Figure 2D, S19). The NOESY relation between δ 2.81 (H-4a) and δ 2.06 (H-5) suggested that these protons were aligned in an equal plane of symmetry, and therefore, arbitrarily positioned as β -protons. However, the proton at δ 1.97 (H-9) did not display any NOESY cross-peaks with the β -oriented protons, and thus, H-9 was assigned to be α -oriented. The IR spectrum of compound **2** displayed the stretching absorptions at 2,925–2,856 and 1732 cm^{-1} that signified the occurrences of alkanes and ester carbonyl functionalities, respectively (Figure S20). The molecular ion peak at m/z 278 ($[M]^+$) appeared to undergo characteristic McLafferty rearrangement to yield the base peak at m/z 74, which might relate to methyl acetate fragment (**2C**) along with a fragment at m/z 206 (**2B**) attributing to 5-(but-10-en-9-yl)-tetrahydro-1*H*-isochromen-3(4*H*)-one (Figures S21–S22). The fragment at m/z 206 (**2B**) underwent McLafferty rearrangement and bond cleavage to form a fragment at m/z 206 (**2D**). The latter on McLafferty rearrangement afforded a peak at m/z 60 (**2E**, acetic acid) along with a fragment at m/z 146 (**2F**, attributed to 2-(but-9-en-8-yl)-6-methylenecyclohexa-1,3-diene), which upon elimination of two methyl radicals yielded a fragment with m/z 120 (**2G**). The repeated elimination of $C_3H_7^{\bullet}$ and $CH_2^{\bullet\bullet}$ radicals from the ion at m/z 1,120 yielded the fragments at m/z 79 (**2H**, attributed to cyclohexa-1, 3-diene) and m/z 67 (**2I**, attributed to penta-1, 3-diene), respectively.

3.3 | Bioactive properties of chromenyl derivatives from *S. inermis*

The antioxidant and antidiabetic properties of (**1–2**) were assessed by DPPH/ABTS⁺ radical scavenging, and the target bioactivities were compared with the commercially available antioxidant α -tocopherol

TABLE 2 In vitro bioactive potentials (antioxidant and antidiabetic) and molecular descriptors (electronic, steric, and hydrophobic)^a of compounds 1–2 from *S. inermis*

Bioactivities					
Antioxidant activity(IC ₅₀ ; mg/ml)	1	2	α-tocopherol		
^a DPPH scavenging activity	0.38 ^a ±0.02	0.51 ^b ±0.01	0.62 ^c ± 0.03		
^a ABTS ⁺ scavenging activity	0.33 ^a ±0.03	0.46 ^b ±0.04	0.54 ^c ±0.01		
Antidiabetic activity (IC ₅₀ ; mg/ml)	1	2	Acarbose		
^a α-amylase inhibition activity	0.27 ^a ±0.03	0.36 ^b ±0.02	0.13 ^c ±0.02		
^a α-glucosidase inhibition activity	0.19 ^a ±0.04	0.28 ^b ±0.01	0.09 ^c ±0.01		
Diprotin A					
^a DPP-IV inhibition activity	0.16 ^a ±0.02	0.23 ^b ±0.03	0.10 ^c ±0.03		
Molecular descriptors					
	1	2	Acarbose	α-tocopherol	Diprotin A
Electronic					
tPSA	74.22	43.37	311.94	29.46	112.73
PI (X10 ⁻²⁴ cm ³)	36.72	30.99	53.45	53.54	35.93
Steric					
MR (cm ³ /mol)	90.4	80.58	134.61	135.06	91.99
MV (cm ³)	312.5	259.6	347.8	462.70	299.4
Pr (cm ³)	791.0	648.0	1,149.4	1,123.00	788.1
Hydrophobic					
Log P _{ow}	1.71	2.16	-6.85	9.98	0.61

Note. tPSA: Topological Polar Surface Area; PI: polarizability; MR: molar refractivity; MV: molar volume; Pr: parachor; Log P_{ow}: logarithm of octanol-water coefficient. The molecular descriptors were calculated using ChemDraw[®] Ultra (CambridgeSoft Corporation, Cambridge, MA, USA; version 8.0) and ACD/ChemSketch (Advanced Chemistry Development, Inc., Canada; version 12.0) software.

^aThe bioactivities were expressed as IC₅₀ values (mg/ml). The samples were analyzed in triplicate (n = 3) and expressed as mean ± SD. Means followed by different superscripts (a–c) within the same row indicated significant differences (p < 0.05).

(Table 2). The hexahydro chromenyl analogue (1) exhibited significantly higher ABTS⁺ and DPPH scavenging properties (IC₅₀ 0.33 and 0.38 mg/ml, respectively) than that possessed by its tetrahydro oxo-isochromenyl chemotype (2) (IC₅₀ 0.46 and 0.51 mg/ml, respectively) (p < 0.05). The antioxidant activity of the chromenyl derivatives were previously reported from the bivalve mollusc (Joy & Chakraborty, 2018), which corroborated the reported free radical scavenging activities of the chromenyl derivatives from the cephalopod mollusc considered in the current study.

The in vitro antihyperglycemic effects of the purified chromenyl chemotypes were determined through the inhibition of carbolytic enzymes α-glucosidase and α-amylase, which reduce the absorption of intestinal carbohydrates, and also inhibit the enzymatic action of DPP-IV, the key regulator in the insulin secretion. Among the compounds, hexahydro chromenyl analogue, 1 exhibited greater α-amylase and α-glucosidase (IC₅₀ 0.27 and 0.19 mg/ml, respectively) inhibiting potential compared to tetrahydro oxo-isochromenyl derivative 2 (IC₅₀ 0.36 and 0.28 mg/ml, respectively). Likewise, the compound 1 showed greater DPP-IV inhibiting activity (IC₅₀ 0.16 mg/ml) compared to that displayed by compound 2 (IC₅₀ 0.23 mg/ml). Inhibitors of the carbolytic enzymes could slow down the liberation of absorbable monosaccharides from the

dietary complex carbohydrates, and could be considered as an effective strategy for the treatment of postprandial hyperglycemic spike by reducing gastrointestinal glucose absorption (Elya et al., 2015). In the current study, the chromenyl derivatives exhibited potential attenuating activities against carbohydrate hydrolyzing enzymes to ameliorate hyperglycemia and associated ailments. Additionally, the efficacy of compound 1 to attenuate insulin secretion regulator DPP-IV appropriately attributed its efficiency as an important natural lead against postprandial hyperglycemia and incretin hormone regulation in addition with the inhibition of active carbohydrate hydrolyzing enzymes α-amylase and α-glucosidase to maintain glucose homeostasis in the biological system.

The physicochemical parameters of the chromenyl chemotypes, 1 and 2 were used to corroborate their free radical scavenging and antihyperglycemic potentials (Table 2). The lipophilic descriptor (log P_{ow}) appeared to guide the inter-membrane permeability of the metabolites, and the optimum value of 1.5–5 was considered to be effective in maintaining a stable hydrophobic-lipophilic balance (Lipinski, 2004). Notably, the hydrophobic property of the studied chromenyl derivatives possessed the optimum log P_{ow} (1.5–2.5) compared with α-tocopherol (log P_{ow} 9.98), acarbose (log P_{ow} -6.85), and diprotin A (log P_{ow} 0.61). Polarizability or electronic system of a molecule

was found to play prominent role in modeling the biological activities (Almi, Belaidi, Lanez, & Tchoua, 2014). The electronic parameter of compound **1**, referred in terms of polarizability (PI), recorded significantly greater value ($PI\ 36.72 \times 10^{-24}\ \text{cm}^3$) compared with those displayed by compound **2** ($PI\ 30.99 \times 10^{-24}\ \text{cm}^3$) and DPP-IV inhibitor diprotin A ($PI\ 35.93 \times 10^{-24}\ \text{cm}^3$). Likewise the topological polar surface area (tPSA) of the compound **1** was greater (tPSA 74.22) as compared to those recorded with **2** (43.37) and standard antioxidant α -tocopherol (29.46), which implied the greater electronic interaction of the former might result in efficient free radical scavenging activities. The lesser bulk (steric) parameters of the studied compounds

($MR < 91\ \text{cm}^3/\text{mol}$; $MV < 320\ \text{cm}^3$; $Pr < 800\ \text{cm}^3$) might contribute toward their greater radical scavenging abilities compared to α -tocopherol ($MV\ 462.70\ \text{cm}^3$; $Pr\ 1,123\ \text{cm}^3$; $MR\ 135.06\ \text{cm}^3$) and higher hyperglycemic potential to commercially available antidiabetic drug acarbose ($MV\ 347.8\ \text{cm}^3$; $Pr\ 1,149.4\ \text{cm}^3$; $MR\ 134.61\ \text{cm}^3$).

3.4 | *In silico* molecular docking analysis of the chromenyl derivatives

The molecular docking analyses of the isolated chromenyl derivatives (**1–2**) were performed against DPP-IV enzyme, and their

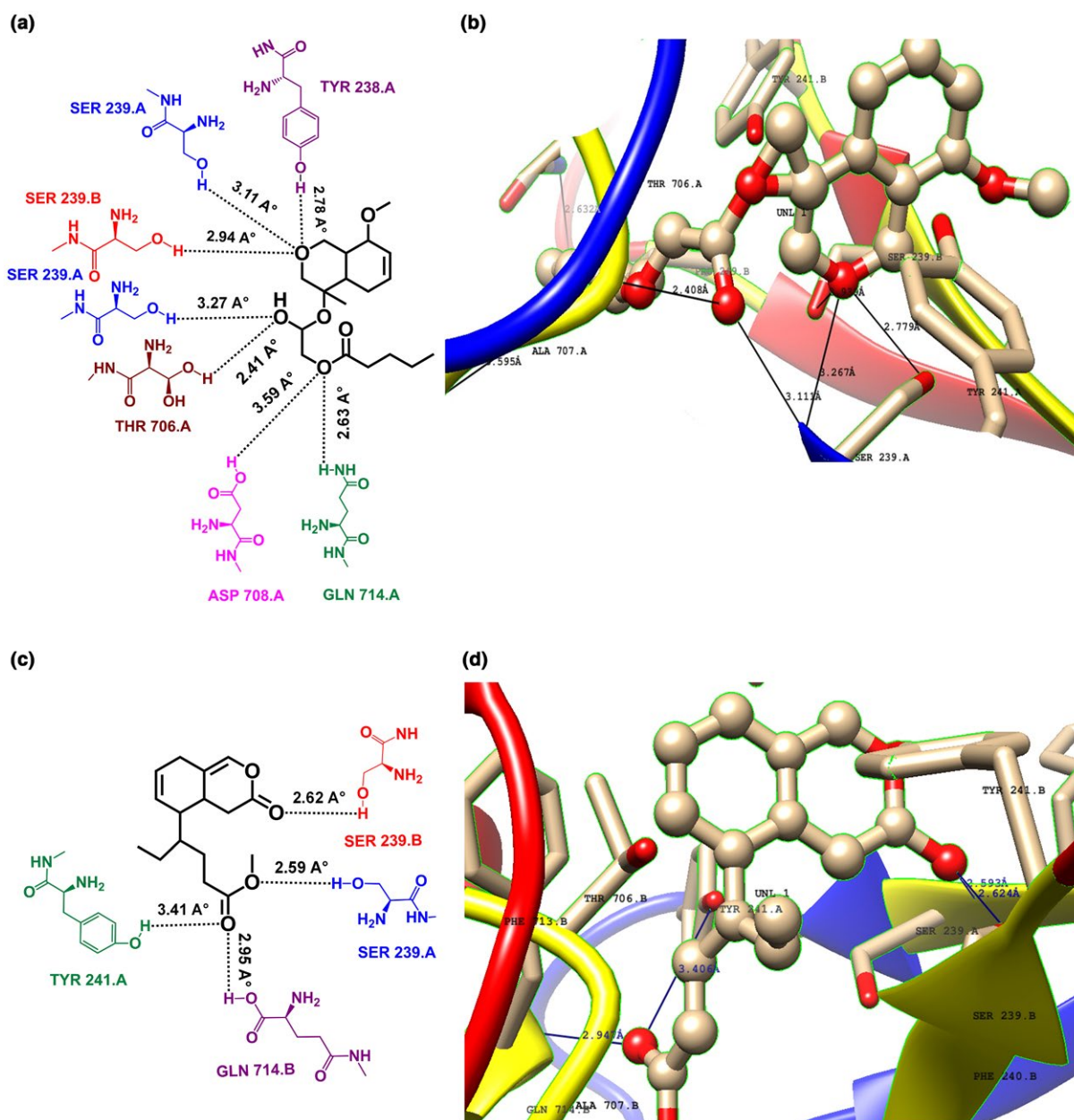


FIGURE 3 Closer view of molecular binding interactions of compounds, **1** (a) and **2** (c) in the binding site of DPP-IV as assessed from the molecular docking simulations. The black colored bond indicated the H-bonding interactions and corresponding distance (Å) with the binding site of molecular target (DPP-IV). Predicted molecular interactions between the chromenyl analogues **1** and **2** with the active site amino acyl residues of DPP-IV (b and d). A representative interaction of the amino acyl residues of DPP-IV, which might interact with the chromenyl analogues **1** and **2**

TABLE 3 Number of hydrogen bonds (H-bonds), hydrogen bonded (H-bonded) amino acid residue and corresponding distance (Å), binding energy, intermolecular energy and inhibition constant between the ligands (compounds 1–2) and the binding sites of DPP-IV

Ligands	No. of H-bonds ^a	H-bonded amino acid residues and corresponding distance Å ^b	Binding energy (kcal/mol) ^c	Intermolecular energy (kcal/mol) ^c	Inhibition constant, K_i (nM) ^c
1	7	ASP 708.A (3.59) THR 706.A (2.41) SER 239.A (3.11) SER 239.A (3.27) TYR 238.A (2.78) SER 239.B (2.94) GLN 714.A (2.63)	-10.01	-11.20	46.41
2	4	SER 239.A (2.59) SER 239.B (2.62) TYR 241.A (3.41) GLN 714.B (2.95)	-8.84	-9.95	329.67

^aMolecular docking simulations were carried out using Autodock 4 software tool. ^bHydrogen bonding interactions between the ligand and the protein complexes. ^cValues were evaluated from the calculations based on the energy minimization.

RMSD results were studied (Figure 3). DPP-IV is a 766 amino acid trans-membrane glycoprotein comprising of cytoplasmic tail (residues 1–6), a trans membrane region (residues 7–28), and an extracellular fragment (29–766). The hydrogen-bonded amino acyl residues and free energy between the chromenyl chemotypes and DPP-IV active sites were recorded (Table 3). In silico molecular docking analyses of chromenyl derivatives with DPP-IV disclosed that the docked ligands could conceivably bind with target, and displayed reduced binding energies (–8.84 and –10.01 kcal/mol). Particularly, the 11-(hexahydro-8-methoxy-4-methyl-1*H*-isochromen-4-yloxy)-11-hydroxyethyl pentanoate derivative (compound 1) registered least binding energy (–10.01 kcal/mol), preceded by that of methyl 9-(tetrahydro-3-oxo-3*H*-isochromen-5-yl) hexanoate isoform (compound 2, –8.84 kcal/mol). The binding energy appeared to reflect the ligand interaction with residues as a principal index to measure inhibitory activity of a ligand (Niu, Gan, Chen, & Feng, 2017). The lesser binding energy of 1 with the enzyme was deduced to be coherent with its higher DPP-IV inhibitory activity (IC₅₀ 0.16 mg/ml). The studied compound 1 exhibited two hydrogen-bonded interactions with one amino acyl residue SER 239.A, and five hydrogen-bonded interactions with ASP 708.A, THR 706.A, TYR 238.A, GLN 714.A (Figure 3a,b). Chromenyl derivative 1 displayed hydrogen-bonded interaction with the catalytic domain (residues 508–766), which showed the α/β hydrolase-fold containing the catalytic triad of SER 630-ASP 708-HIS 740 (Kuhn, Hennig, & Mattei, 2007). The chromenyl derivative 2 displayed four hydrogen bonds with SER 239.A, SER 239.B, TYR 241.A, GLN 714.A (Table 3) (Figure 3c,d). Additionally, the distance of hydrogen bonds between the studied compounds (1–2) and molecular receptor of DPP-IV were deduced to be lesser than 3.5 Å, which appropriately recognized their effective binding properties to form ligand–protein complex (Girgih, He, & Aluko, 2014). In the current study, the ligand (1) exhibited a binding energy of –10.01 kcal/mol, which was found to be comparable with the commercially available DPP-IV inhibitors namely, vigildagliptin (–7.43 kcal/mol), and linagliptin (–7.91 kcal/mol) with DPP-IV protein target (Anitha, Gopi, Girish, & Kumar, 2013). The inhibition constants, K_i and intermolecular energy were found to be lesser for compound 1 (46.41 nM and –11.20 kcal/mol, respectively) than those exhibited by compound 2 (329.67 nM and –9.95 kcal/mol). These results appropriately corroborated the greater enzyme inhibition activities of the chromenyl derivative with 1*H*-isochromenyloxy-11-hydroxyethyl pentanoate moiety (compound 1) than that bearing 3*H*-isochromenyl hexanoate framework (compound 2) against the key regulator of insulin secretion DPP-IV.

4 | CONCLUSIONS

Two chromenyl analogues were isolated from the spineless cuttlefish, *Sepiella inermis*, and their chemistries were deduced by extensive spectroscopic experiments. The potential antioxidant and inhibitory activities of the chromenyl analogue

with 1*H*-isochromenyloxy-11-hydroxyethyl pentanoate framework against serine protease dipeptidyl peptidase-IV, a key regulator of blood glucose level and endogenous active glucagon-like peptide-1, signified its utilities as potential functional food ingredient. The greater antihyperglycemic properties of the 1*H*-isochromenyloxy derivative were ascribed by its optimum hydrophilic-lipophilic balance along with lesser steric bulk for favorable interaction with the active site amino acyl residues of dipeptidyl peptidase-IV leading to least binding energy of -10.01 kcal/mol. The recognition of potential antihyperglycemic properties of the chromenyl metabolites isolated from *S. inermis* appropriately recognized their potential as naturally occurring lead molecules in the functional food formulations.

ACKNOWLEDGMENTS

The authors are thankful to the Indian Council of Agricultural Research-funded Consortium Research Platform Project on "Health Food" (ICAR/HF/2012-2017). The authors are grateful to the Director, Central Marine Fisheries Research Institute and Head, Marine Biotechnology Division of the institute to facilitate the research activities. S.K. and M.J. thanks Indian Council of Agricultural Research for fellowships.

CONFLICT OF INTEREST

The authors declared that they have no conflict of interest.

ORCID

Kajal Chakraborty  <https://orcid.org/0000-0002-7105-8942>

REFERENCES

- Almi, Z., Belaidi, S., Lanez, T., & Tchouar, N. (2014). Structure activity relationships, QSAR modeling and drug-like calculations of TP inhibition of 1,3,4 oxadiazoline-2-thione derivatives. *International Letters of Chemistry, Physics and Astronomy*, *37*, 113–124. <https://doi.org/10.18052/www.scipress.com/ILCPA.37.113>
- Ammirati, M. J., Andrews, K. M., Boyer, D. D., Brodeur, A. M., Danley, D. E., Doran, S. D., ... Piotrowski, D. W. (2009). (3,3-Difluoro-pyrrolidin-1-yl)-[(2*S*,4*S*)-(4-(4-pyrimidin-2-yl-piperazin-1-yl)-pyrrolidin-2-yl)-methanone: A potent, selective, orally active dipeptidyl peptidase IV inhibitor. *Bioorganic and Medicinal Chemistry Letters*, *19*, 1991–1995. <https://doi.org/10.1016/j.bmcl.2009.02.041>
- Anitha, K., Gopi, G., & Girish, K. P. S. (2013). Molecular docking study on dipeptidyl peptidase-4 inhibitors. *International Journal of Research and Development in Pharmacy and Life Sciences*, *2*, 602–610.
- Appleton, D. R., Sewell, M. A., Berridge, M. V., & Copp, B. R. (2002). A new biologically active malyngamide from a New Zealand collection of the sea hare *Bursatella leachii*. *Journal of Natural Products*, *65*, 630–631. <https://doi.org/10.1021/np010511e>
- Chakraborty, K., & Joy, M. (2016). Anti-diabetic and anti-inflammatory activities of commonly available cephalopods. *International Journal of Food Properties*, *20*, 1655–1665. <https://doi.org/10.1080/10942912.2016.1217008>
- Chakraborty, K., Joy, M., & Vijayagopal, P. (2016). Nutritional qualities of common edible cephalopods at the Arabian Sea. *International Food Research Journal*, *23*, 1926–1938.
- El-Beih, A. A., Kato, H., Ohta, T., & Tsukamoto, S. (2007). (3*R*,4*aR*,5*S*,6*R*)-6-Hydroxy-5-methylramulosin: A new ramulosin derivative from a marine-derived sterile mycelium. *Chemical and Pharmaceutical Bulletin*, *55*, 953–954. <https://doi.org/10.1248/cpb.55.953>
- Elya, B., Handayani, R., Sauriasari, R., A., Hasyiyati, U. S., Permana, I. T., & Permatasar, Y. I. (2015). Anti-diabetic activity and phytochemical screening of extracts from Indonesian plants by inhibition of alpha amylase, alpha glucosidase and dipeptidyl peptidase IV. *Pakistan Journal of Biological Sciences*, *18*, 279–284. <https://doi.org/10.3923/pjbs.2015.279.284>
- Girgih, A. T., He, R., & Aluko, R. E. (2014). Kinetics and molecular docking studies of the inhibitions of angiotensin converting enzyme and renin activities by hemp seed (*Cannabis sativa* L.) peptides. *Journal of Agricultural and Food Chemistry*, *62*, 4135–4144. <https://doi.org/10.1021/jf5002606>
- Hamdan, I. I., & Afifi, F. U. (2004). Studies on the *in vitro* and *in vivo* hypoglycemic activities of some medicinal plants used in treatment of diabetes in Jordanian traditional medicine. *Journal of Ethnopharmacology*, *93*, 117–121. <https://doi.org/10.1016/j.jep.2004.03.033>
- Joy, M., & Chakraborty, K. (2017). Previously undescribed antioxidative and anti-inflammatory chromenyls bearing 3*H*-isochromenone and furanyl-2*H*-chromenyl skeletons from the venerid clam, *Paphia malabarica*. *Medicinal Chemistry Research*, *26*, 1708–1722. <https://doi.org/10.1007/s00044-017-1886-x>
- Joy, M., & Chakraborty, K. (2018). Anti-oxidative and anti-inflammatory pyranoids and isochromenyl analogues from Corbiculid bivalve clam, *Villorita cyprinoides*. *Food Chemistry*, *251*, 125–134. <https://doi.org/10.1016/j.foodchem.2018.01.059>
- Kojima, K., Hama, T., Kato, T., & Nagatsu, T. (1980). Rapid chromatographic purification of dipeptidyl peptidase-IV in human submaxillary gland. *Journal of Chromatography A*, *189*, 233–240. [https://doi.org/10.1016/s0021-9673\(00\)81523-x](https://doi.org/10.1016/s0021-9673(00)81523-x)
- Kuhn, B., Hennig, M., & Mattei, P. (2007). Molecular recognition of ligands in dipeptidyl peptidase IV. *Current Topics in Medicinal Chemistry*, *7*, 609–619. <https://doi.org/10.2174/156802607780091064>
- Lin, T., Wang, G. H., Lin, X., Hu, Z. Y., Chen, Q. C., Xu, Y., ... Chen, H. F. (2011). Three new oblongolides from *Phomopsis* sp. XZ-01, an endophytic fungus from *Camptotheca acuminata*. *Molecules*, *16*, 3351–3359. <https://doi.org/10.3390/molecules16043351>
- Lipinski, C. A. (2004). Lead and drug-like compounds: The rule-of-five revolution. *Drug Discovery Today Technologies*, *1*, 337–341. <https://doi.org/10.1016/j.ddtec.2004.11.007>
- Mitra, A., Dewanjee, D., & Dey, B. (2012). Mechanistic studies of lifestyle interventions in type 2 diabetes. *World Journal of Diabetes*, *3*, 201–207. <https://doi.org/10.4239/wjd.v3.i12.201>
- Niu, E., Gan, Q., Chen, X., & Feng, C. (2017). Sulfonamide-containing PTP 1*B* inhibitors: Docking studies, synthesis and model validation. 2016 International conference on materials science, resource and environmental engineering. *AIP Conference Proceedings*, *1794*, 050003–1–050003-10. <https://doi.org/10.1063/1.4971949>
- Odeleye, T., Li, Y., White, W. L., Nie, S., Chen, S., Wang, J., & Lu, J. (2016). The antioxidant potential of the New Zealand surf clams. *Food Chemistry*, *204*, 141–149. <https://doi.org/10.1016/j.foodchem.2016.02.120>
- Purnomo, Y., Soeatmadji, D. W., Sumitro, S. B., & Widodo, M. A. (2015). Anti-diabetic potential of *Urena lobata* leaf extract through inhibition of dipeptidyl peptidase IV activity. *Asian Pacific Journal of Tropical Biomedicine*, *5*, 645–649. <https://doi.org/10.1016/j.apjtb.2015.05.014>
- Ramasamy, P., Subhapradha, N., Sudharsan, S., Seedeve, P., Shanmugam, V., & Shanmugam, A. (2012). Nutritional evaluation of the different body parts of cuttlefish *Sepia kobeensis* Hoyle, 1885. *African Journal of Food Science*, *6*, 535–538. <https://doi.org/10.5897/AJFS12.069>

- Reid, A., Jereb, P., & Roper, C. F. E. (2005). Family Sepiidae. In P. Jereb & C. F. E. Roper (Eds.), *Cephalopods of the world. An annotated and illustrated catalogue of species known to date. Volume 1. Chambered nautilus and sepioids (Nautilidae, Sepiidae, Sepiolidae, Sepiadariidae, Idiosepiidae and Spirulidae)*. FAO Species Catalogue for Fishery Purposes (pp. 57–152). Rome, Italy: FAO.
- Singh, A. K., Jatwa, R., Purohit, A., & Ram, H. (2017). Synthetic and phytocompounds based dipeptidyl peptidase-IV (DPP-IV) inhibitors for therapeutics of diabetes. *Journal of Asian Natural Products Research*, 19, 1036–1045. <https://doi.org/10.1080/10286020.2017.1307183>
- Ullah, A., Khan, A., & Khan, I. (2016). Diabetes mellitus and oxidative stress-A concise review. *Saudi Pharmaceutical Journal*, 24, 547–553. <https://doi.org/10.1016/j.jsps.2015.03.013>
- Wang, Y., Li, L., Yang, M., Liu, H., Boden, G., & Yang, G. (2011). Glucagon-like peptide-1 receptor agonist versus insulin in inadequately controlled patients with type 2 diabetes mellitus: A meta-analysis of clinical trials. *Diabetes, Obesity and Metabolism*, 13, 972–981. <https://doi.org/10.1111/j.1463-1326.2011.01436.x>
- Wojdylo, A., Oszmiański, J., & Czemyers, R. (2007). Antioxidant activity and phenolic compounds in 32 selected herbs. *Food Chemistry*, 105, 940–949. <https://doi.org/10.1016/j.foodchem.2007.04.038>
- Zhang, D., Tao, X., Chen, R., Liu, J., Li, L., Fang, X., ... Dai, J. (2015). Pericoannosin-A, a polyketide synthase-nonribosomal peptide synthetase hybrid metabolite with new carbon skeleton from the endophytic fungus *Periconia* sp. *Organic Letters*, 17, 4304–4307. <https://doi.org/10.1021/acs.orglett.5b02123>

SUPPORTING INFORMATION

Additional supporting information may be found online in the Supporting Information section at the end of the article.

How to cite this article: Krishnan S, Chakraborty K, Joy M. First report of chromenyl derivatives from spineless marine cuttlefish *Sepiella inermis*: Prospective antihyperglycemic agents attenuate serine protease dipeptidyl peptidase-IV. *J Food Biochem*. 2019;e12824. <https://doi.org/10.1111/jfbc.12824>